nature ecology & evolution

ARTICLES

PUBLISHED: 24 APRIL 2017 | VOLUME: 1 | ARTICLE NUMBER: 0144

A submarine volcanic eruption leads to a novel microbial habitat

Roberto Danovaro[1,2*], Miquel Canals[3], Michael Tangherlini[1], Antonio Dell'Anno[1], Cristina Gambi[1], Galderic Lastras[3], David Amblas[3,4], Anna Sanchez-Vidal[3], Jaime Frigola[3], Antoni M. Calafat[3], Rut Pedrosa[3], Jesus Rivera[5], Xavier Rayo[3] and Cinzia Corinaldesi[6]

Submarine volcanic eruptions are major catastrophic events that allow investigation of the colonization mechanisms of newly formed seabed. We explored the seafloor after the eruption of the Tagoro submarine volcano off El Hierro Island, Canary Archipelago. Near the summit of the volcanic cone, at about 130 m depth, we found massive mats of long, white filaments that we named Venus's hair. Microscopic and molecular analyses revealed that these filaments are made of bacterial trichomes enveloped within a sheath and colonized by epibiotic bacteria. Metagenomic analyses of the filaments identified a new genus and species of the order Thiotrichales, *Thiolava veneris*. Venus's hair shows an unprecedented array of metabolic pathways, spanning from the exploitation of organic and inorganic carbon released by volcanic degassing to the uptake of sulfur and nitrogen compounds. This unique metabolic plasticity provides key competitive advantages for the colonization of the new habitat created by the submarine eruption. A specialized and highly diverse food web thrives on the complex three-dimensional habitat formed by these microorganisms, providing evidence that Venus's hair can drive the restart of biological systems after submarine volcanic eruptions.

Most of the volcanic activity on Earth occurs in the oceans[1,2]. However, available information on the biological processes that enable recolonization of the seafloor after submarine volcanic eruptions is limited[2]. In 138 days (from October 2011 to March 2012), the submarine eruption of Tagoro Volcano, off El Hierro Island, in the northeast Atlantic Ocean, reshaped more than 9 km^2 of the seafloor[3]. The eruption formed a volcanic cone that raised the seafloor from about 363 m up to 89 m of water depth[3]. Floating lava balloons (that is, low-viscosity alkaline lava fragments with high volatile content brought to the sea surface) were also observed. The eruption led to an abrupt increase in water temperature and turbidity, a decrease of oxygen concentration and a massive release of CO_2 and H_2S[4,5], causing a pronounced decrease of primary producers and increase in fish mortality[4], with cascading effects on biogeochemical processes[4–6]. Similar events reported in the East Pacific Rise and Juan de Fuca Ridge also caused major biological effects[7,8]. However, in contrast to systems from mid-ocean ridges and other volcanic areas, such as the Kermadec and Mariana arcs, the Tagoro Volcano is an example (another includes Loihi Volcano in the Hawaiian archipelago)[9,10] of an isolated vent system unconnected to any other known active hydrothermal or volcanic site[3,11–14]; this makes it different from ocean ridge-vent systems, where colonization of the newly formed seafloor after an eruption can be favoured by the nearby presence of other vent assemblages. The Tagoro Volcano eruption thus offered a relevant opportunity to investigate the colonization of new volcanic seafloor in an area without pre-existing hydrothermal vents and associated assemblages.

Results and discussion

First, we provide the taxonomic outline of the new candidate bacterial genus and species (Fig. 1).

Danovaro *et al.*, 2017
Class Gammaproteobacteria (Garrity *et al.*, 2005)
Order Thiotrichales (Garrity *et al.*, 2005)
Family Thiotrichaceae (Garrity *et al.*, 2005)
Thiolava veneris gen. et sp. nov.

Etymology. Genus name from *thio* (Greek), referring to sulfur as the key substrate for the energetic metabolism, and *lava* (Latin), referring to the typology of substrate where the bacteria were discovered. Species name from *veneris* (Latin), genitive of Venus, the ancient Roman goddess of beauty and love.
Locality. Hierro island, Canary Archipelago (Spain).
Diagnosis. Marine filamentous bacterium forming a gelatinous sheath, attached to rock surface. White filaments formed by the bacterium are up to 3 cm long. Filaments create a massive microbial mat on the lava substrate.
Source of type material. No viable deposit available. Genome completeness 82%.

Here we show that the most severely impacted area (Supplementary Fig. 1), 32 months after the eruption, was colonized by a massive mat of white filaments that were up to a few centimetres long (Supplementary Fig. 2) and attached to the lava substrate, which we named Venus's hair, because of its macroscopic characteristics. Remotely operated vehicle (ROV) surveys highlighted that the microbial mat extended for about 2,000 m^2 around the summit of the newly formed Tagoro volcanic cone, at depths ranging from 129 to 132 m (Supplementary Fig. 1). The dark and highly porous volcanic rocks and lapilli, where these filaments were found, are basanitic lavas primarily composed of silicates (~42% w-w in the form of quartz), iron (~14%, as iron oxide), aluminium (~13%, as aluminium oxide), calcium and magnesium (~11% and ~8%, as

[1]Department of Life and Environmental Sciences, Polytechnic University of Marche, Ancona 60131, Italy. [2]Stazione Zoologica Anton Dohrn, Naples, Naples 80121, Italy. [3]CRG Marine Geosciences, Department of Earth and Ocean Dynamics, Faculty of Earth Sciences, University of Barcelona, Barcelona E-08028, Spain. [4]Scott Polar Research Institute, Lensfield Road, Cambridge, UK. [5]Instituto Español de Oceanografía, Corazón de María 8, Madrid E-28002, Spain. [6]Dipartimento di Scienze e Ingegneria della Materia, dell'Ambiente ed Urbanistica, Polytechnic University of Marche, Ancona 60131, Italy. *e-mail: r.danovaro@univpm.it

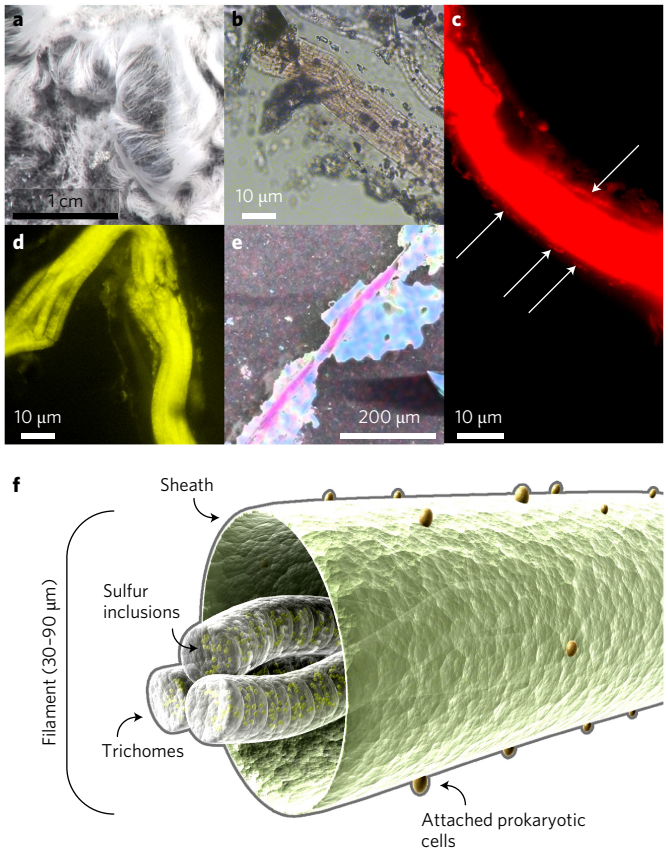

Figure 1 | Macroscopic and microscopic view of the Venus's hair. a, ROV close-up of a portion of the Venus's hair microbial mat. **b**, Photograph obtained by light microscopy of a single *Thiolava veneris* filament at ×400 magnification, showing its overall structure. **c**, Epifluorescence micrograph of a single *T. veneris* filament at ×400 magnification after hybridization with the Bacterial CARD-FISH probe; arrows highlight the presence of several smaller cells attached to the sheath (small dots). **d**, Epifluorescence micrograph of a single *T. veneris* filament at ×400 magnification after hybridization with the Bacterial CARD-FISH probe, highlighting the structure of the trichomes. **e**, SEM photograph of a single *T. veneris* small filament, showing the distribution of sulfur on the filament (purple). **f**, Reconstruction of the structure of a *T. veneris* filament, showing the external sheath, the trichomes and their internal sulfur inclusions.

calcium oxide and manganese oxide, respectively), and titanium (~4.6%, as titanium dioxide) (Supplementary Tables 1 and 2). Such a composition of the lavas is very similar to sample EH BASAN (El Hierro basanite)[15], with practically the same contents of the major elements. In spite of this, samples show a large variability in their sulfur content (from 0.01 to 0.25% w-w), which suggests the release of volatile sulfur compounds (that is, sulfur dioxide and hydrogen sulfide) during volcanic degassing and an extensive release of CO_2, accounting for 0.1% of the global volcanic CO_2 emissions[16].

Detailed analyses of the Venus's hair filaments carried out by light and epifluorescence microscopy (including fluorescence *in situ* hybridization analysis) and scanning electron microscopy (SEM) revealed that the filaments are formed by long trichomes of contiguous bacterial cells (diameter ranging from 3 to 6 µm) within a 36 to 90 µm-wide sheath colonized by bacteria (Fig. 1). These filaments are similar to those formed by members of the genus *Thioploca*[17], but Venus's hair is firmly attached to the substrate, whereas the *Thioploca* filaments are not and can move through the sediment. In addition, SEM and energy-dispersive X-ray spectroscopy (SEM–EDX), and X-ray fluorescence spectrometry analyses identified sulfur as the major inorganic element contained in the filaments (up to 0.008 pmol µm^{-3}) (Fig. 1). High sulfur contents also have been reported in sulfur-oxidizing filamentous Thiotrichales, including the genera *Beggiatoa* and *Thioploca*, whose metabolisms are fuelled by sulfur inorganic species released by geothermal fluids and/or by sulfate reduction processes[18–20]. However, Venus's hair, in contrast to all other Thiotrichales identified so far, does not contain vacuoles.

Metagenomic analysis of DNA from the filaments allowed us also to reconstruct 21 partial genomes with an estimated completeness >80%, 16 of which affiliated with Proteobacteria and the remaining 5 with Bacteroidetes (Fig. 2 and Supplementary Table 3). Results of the phylogenomic analyses carried out on multiple specific gene markers showed that bin 11 (completeness 82%), affiliated to the family Thiotrichaceae (class Gammaproteobacteria), dominated all reads (Fig. 2). The highest similarity (~78% of average nucleotide identity) was observed with the draft genome of the filamentous *Thioploca araucae*, sharing with this organism 1,105 of its 3,191 predicted proteins (equivalent to 34%) with an average amino acid identity of 51%. The large genomic and functional differences between bin 11 and its closest relative within the same family indicate that the bacteria that form the Venus's hair filaments can be a candidate for a new genus and species (Candidatus *Thiolava veneris*). The lack of ribosomal genes in the sequences contained within bin 11 hampered the design of specific probes for the fluorescence *in situ* hybridization analysis on intact filaments.

Analysis of the metabolic potential revealed that the genome of Candidatus *Thiolava veneris* contains genes involved in the tricarboxylic acid cycle (except for the lack of the genes encoding for malate dehydrogenase; Fig. 3) for the exploitation of organic substrates and those involved in three different CO_2 fixation pathways: (1) the Calvin–Benson–Bassham cycle, (2) the reductive tricarboxylic acid cycle and (3) the C4-dicarboxylic acid cycle (Fig. 3). The genome of *Thiolava veneris* also contains genes involved in different pathways of sulfur metabolism (that is, dissimilatory sulfur oxidation from H_2S to SO_4^{2-} and the oxidation of thiosulfate through the sulfur-oxidation (Sox) pathway; Fig. 3). At the same time, the apparent lack of the sulfane dehydrogenase (SoxCD) step in the thiosulfate oxidation pathway suggests that the oxidation of elemental sulfur (S^0) to sulfite is not performed in the periplasmic space, as occurs in other Thiotrichales[20], but in the cytoplasm. We cannot exclude the possibility that the SoxCD step is lacking due to an incomplete genome reconstruction. However, if these results were confirmed, this missing step could represent a strategy to allow these bacteria to store sulfur within the cell, without producing vacuoles (typically present in other bacteria storing sulfur), and to perform thiosulfate oxidation very efficiently, a feature also recently reported for sulfur-oxidizing facultative anaerobic bacteria[20]. The sulfur storage capacity of *Thiolava veneris* was confirmed by SEM–EDX and total X-ray fluorescence (TXRF) analyses (Fig. 1). The presence of genes for both dissimilatory (in periplasm) and assimilatory (in cytoplasm) nitrate reduction (that is, from NO^{3-} to NH_3)[18–20] (Fig. 3) indicates that inorganic nitrogen compounds are used by *Thiolava veneris* not only as terminal electron acceptors (that is, NO^{3-}) required for sulfur oxidation, but also as a source (that is, NH_3) for biosynthetic pathways. Moreover, these bacteria possess genes that encode oxygen-tolerant NiFe hydrogenases, which can be involved in the recycling of oxidized sulfur compounds and energy generation through molecular hydrogen[21]. Comparison of the metabolic pathways of *Thiolava veneris* with those available in the KEGG database revealed that the combination of metabolic pathways for inorganic carbon assimilation has never been reported for any bacterial genome (comparison with Thiotrichales is shown in Fig. 3)[22–24].

The partial genome of *Thiolava veneris* also contains a gene that encodes a protein showing 60% similarity with a known heavy metal-translocating ATPase, which could be used for detoxification

of metals (for example, titanium) leached from the solidified lavas (due to the reducing conditions of the system)[25]. The other genomic bins reconstructed from the filament also revealed the presence of a wide array of metabolic pathways, including those for CO_2 fixation and the degradation of organic matter[26]. This is coherent with the high extracellular enzymatic activities observed on the filament,

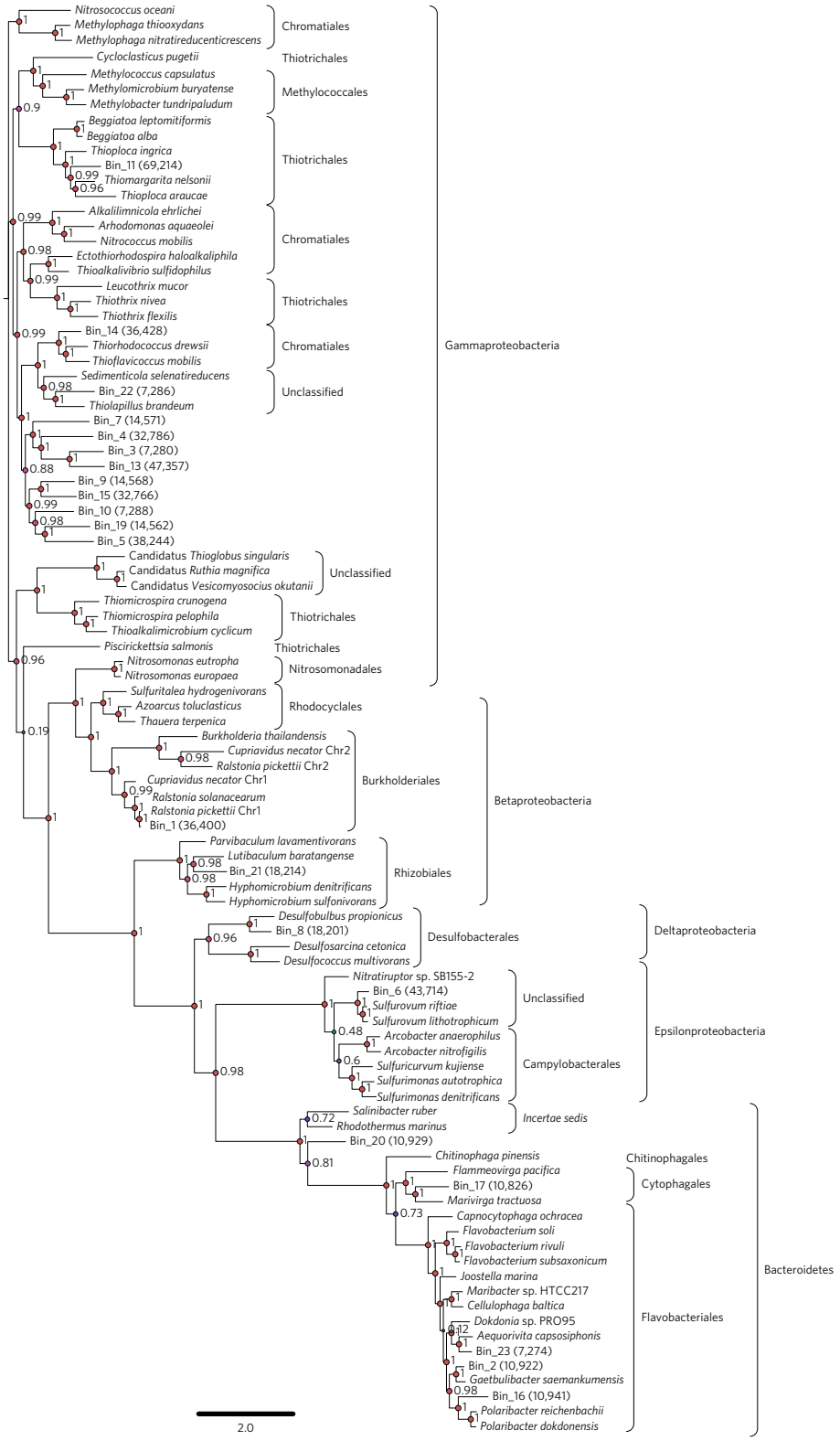

Figure 2 | Phylogenomic analyses on genome bins reconstructed from the Venus's hair metagenome. Phylogenomic tree constructed on multiple gene markers showing all the genome bins reconstructed in the present study and prokaryotic genomes belonging to the same classes. The size and colour of the circles at the branch points correspond to the branch support values, which are also reported as numbers. Bin 11 refers to the partial genome of *Thiolava veneris*. The number of reads (after quality check) for each bin are reported in parentheses.

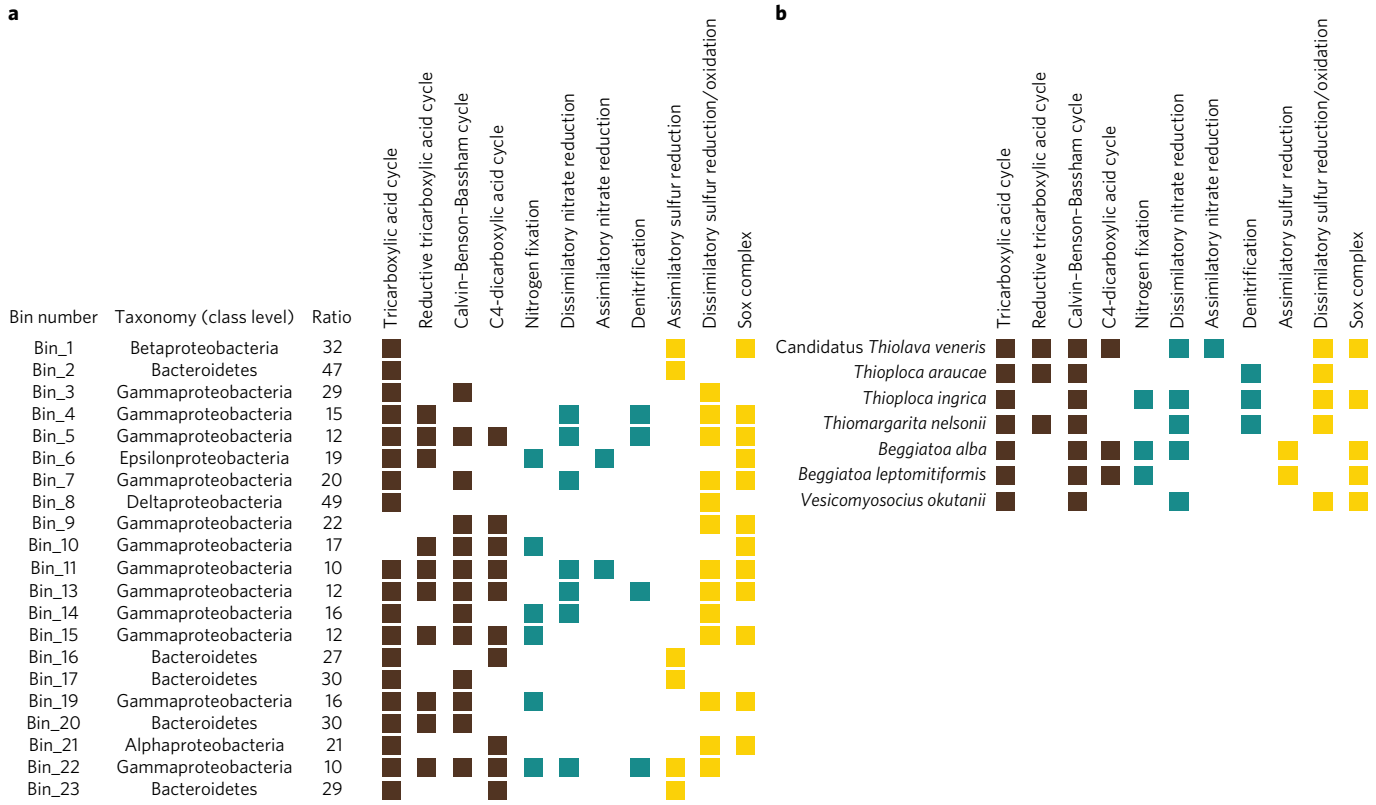

Figure 3 | Metabolic potential of *Thiolava veneris*. a, Metabolic pathways for organic and inorganic carbon utilization and nitrogen and sulfur metabolism identified in each genomic bin reconstructed in the present study. The numbers reported as 'Ratio' represent the ratio of genome completeness to the number of identified metabolic pathways. **b**, Comparison of metabolic pathways identified in *T. veneris* and similar prokaryotic genomes.

which might include both heterotrophic activity by *Thiolava veneris* and from the bacteria colonizing the sheaths (~21 and 31 nmol g^{-1} h^{-1} for alkaline phosphatases and aminopeptidases, respectively; Supplementary Fig. 3). None of the genomic bins identified contained genes associated with photosynthetic pathways, therefore excluding photosynthesis from the metabolism of Venus's hair filaments (including Candidatus *Thiolava veneris*)[27].

Bioinformatic analyses indicated that the assemblage associated with the Venus's hair filaments is completely different, and indeed segregated apart, from any other assemblage reported from hydrothermal systems or elsewhere to date (Supplementary Table 4 and Supplementary Fig. 4). In particular, the comparison among metagenomes (Supplementary Fig. 4) showed that the similarity (in terms of k-mer frequency) between the Venus's hair and other microbial assemblages considered is lower than 0.1%. Although such a comparison should be viewed with caution, due to the limited number of metagenomes and the variable presence of eukaryotic and viral sequences contained therein, these results suggest that Venus's hair is not only macroscopically different from known vent assemblages, but also very different from a phylogenetic and ecological point of view.

Overall, the results of microscopy, phylogenetic, phylogenomic and functional analyses carried out on the *Thiolava veneris* filaments suggest that the filaments are characterized by a unique combination of pathways that enhance their metabolic efficiency and tolerance to metal exposure. Moreover, the filamentous structure characterized by long trichomes of contiguous cells can be seen as a successful strategy for the colonization of volcanic substrates; the sessile strategy allows the microorganisms to remain permanently in close proximity to the volcanic seepage, with continuous access to essential elements required for their metabolism. In addition, the sheathed structure, the strong mechanical resistance and the chemical properties of the filaments might limit their grazing by protists or metazoans. All of these features provide advantages for the massive colonization of the new habitat created by the submarine eruption. However, since *Thiolava veneris* has been reported and described here for the first time, it is difficult to explain the origin and spreading mechanisms of these microorganisms. Further studies are needed to clarify how these organisms spread.

The three-dimensional structure of the Venus's hair mat favours the establishment of a complex food web following the submarine volcanic eruption. Indeed, the Venus's hair mat represents a substrate for the colonization of a variety of organisms. High-throughput sequencing of 16S and 18S rRNA genes of the entire microbial mat attached to the basanitic lavas revealed the presence of a diversified assemblage of prokaryotes and multicellular eukaryotes (metazoans). Among Bacteria, Epsilonproteobacteria accounted for 55% of all bacterial sequences, followed by Gammaproteobacteria and Alphaproteobacteria (both approximately 10%; Fig. 4). Archaea provided a negligible contribution (0.03%). The most abundant genera of the mat were *Sulfurimonas* and *Sulfurovum* (39% and 14% of the total sequences, respectively), which are Epsilonproteobacteria. The relatively low contribution of the 16S rRNA genes belonging to Thiotrichales (Gammaproteobacteria), which contributed a large majority of the reads obtained by metagenomic analysis, is probably due to the different strategy utilized for the analyses of the microbial assemblages (that is, single filaments analysed by shotgun sequencing versus whole mat analysed by amplicon sequencing). The prokaryotic assemblages of the mat were completely different from those of hydrothermal vent ecosystems investigated so far and even those from the seawater samples surrounding the lava substrate (Fig. 4). Only the prokaryotic assemblages from the Woody Crack Front vent site, located in the Mid-Atlantic Ridge showed ~15% similarity with those of the Tagoro's mat.

We found sequences of metazoan taxa belonging to meiofauna (for example, arthropods, annelids and nematodes; Supplementary Fig. 5) that were characterized by different trophic strategies, from grazers and epistrate-feeders to predators. In addition, the mat contained the larvae and juvenile stages of benthic fauna, providing evidence that Venus's hair can also sustain the entire life cycle of the smallest benthic metazoan organisms, for which microorganisms could represent an important food resource[28]. The results of the

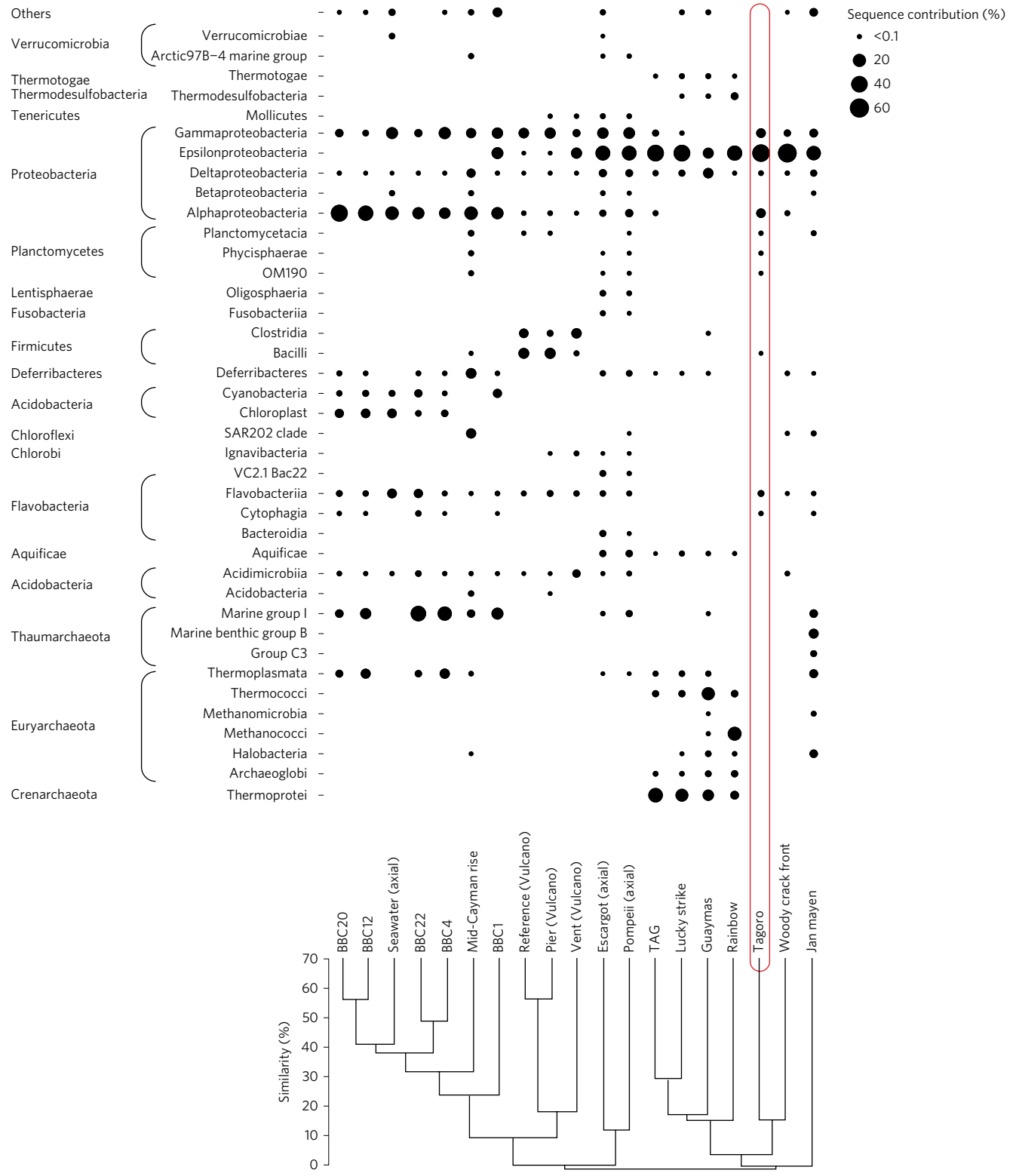

Figure 4 | Output of prokaryotic 16S rDNA sequencing. Circle heatmap representing the contribution of prokaryotic taxa to the assemblage of the Venus's hair mat compared with that of other hydrothermal vent metagenomes and those representing the water column above and around the eruption area (BBC1, 4, 12, 20, 22). Circle sizes refer to the percentage contribution of sequences to classes. The dendrogram represents the similarity distance among samples based on Bray–Curtis similarity analysis.

molecular analyses revealed the presence of known nematode species (for example, *Paracanthonchus*) that are also found in hydrothermal vent systems[27,29] and arthropods (Supplementary Fig. 6). However, the fact that most of the species found remain unassigned (5,100 unmatched operational taxonomic units (OTU)) suggests the presence of a large number of new species not included in current databases and provides an important contribution to biodiversity at the regional scale.

Conclusions

Our findings show that the peculiar metabolic characteristics of the Venus's hair microbial assemblage allowed it to colonize the newly formed seabed resulting from isolated submarine volcanic eruptions. This paved the way for the development of early-stage ecosystems and the consequent subsistence of metazoans and higher trophic levels. The information gathered from Tagoro Volcano provides novel insights into understanding the restart of life after catastrophic events, such as submarine volcanic eruptions, and the creation of new habitats hosting extensive and previously unknown biodiversity.

Methods

Sampling area and sample collection. The filamentous microbial mats were discovered and sampled during the MIDAS El Hierro 2014 expedition to investigate the eventual recovery of the benthic ecosystem after the 2011–2012 submarine volcanic eruption off El Hierro. The cruise took place from 28 October to 17 November onboard RV *Ángeles Alvariño*. Numerous dives were performed with the *Super-Mohawk II 'Liropus 2000'* ROV from Instituto Español de Oceanografía. Among other instruments, the ROV was equipped with a frontal full high-definition Kongsberg OE14-502A colour camera, two manipulators (HLK-HD45 5Func and HLK-47000 6Func, Hydro-Lek), a conductivity, temperature and depth (CTD) SBE 37 Microcat (Sea Bird Scientific), two 532 nm laser pointers, a sampling skid, a dual frequency sonar (325 kHz and 675 kHz, Super SeaKing DST), an altimeter and an acoustic beacon (MST 324, Konsberg). Samples of the filamentous mats and the substratum on which they were growing were carefully collected with the ROV manipulators using a guided grab sampler from 129 to 132 m of water depth, between latitudes 27° 37.169′ N and 27° 37.190′ N, and longitudes 17° 59.615′ W and 17° 59.620′ W. Immediately after collection, the samples were sealed *in situ*, and once onboard were placed in sterile jars and frozen for subsequent laboratory analyses. A portion of the filaments collected was used immediately after collection (onboard the RV) for the analysis of the extracellular enzymatic activities.

Geochemical analysis of substrate rocks. Elemental geochemical analyses of rock samples were performed by inductively couple plasma–optical emission spectrometry (ICP–OES) and ICP–mass spectrometry (ICP–MS), and analyses of oxides were carried out by X-ray fluorescence. For the elemental analyses, 100 mg of each powdered rock sample was digested with 2 ml of 65% HNO_3 in closed Teflon beakers at 90 °C overnight. After cooling down at room temperature, the sample digests were centrifuged and rinsed with HNO_3, then 1 ml of 65% HNO_3 and 5 ml of 40% HF were added and the samples were left at 90 °C overnight. Then, 2 ml of 70% $HClO_4$ was added to each sample and evaporated on a hot plate in a specially designed $HClO_4$ fume hood; this was repeated twice. Samples were redissolved with 65% HNO_3 and heated again for 30 min. Samples were cooled and diluted with Milli-Q water, and analysed using an ICP–OES system for K, Na, P, Mn, S, Ti, Ba, Al, Ca, Mg and Fe, and a PerkinElmer Elan-6000 ICP–MS system for As, Cu, Zn, Ti, Se, Ag, Te and Ce. For the analysis of oxides, 300 mg of each powdered rock sample was fused at high temperature (>1,000 °C) with 600 mg of lithium tetraborate. Oxides of Al, Ca, Fe, K, Mg, Mn, Na, P, Si and Ti were determined using a PANalytical PW 4400/40 X-ray fluorescence spectrophotometer (WDXRF).

Light and epifluorescence microscopy. Venus's hair filaments were hand-picked with a sterile steel pick under a Zeiss stereomicroscope and placed on a glass slide in a drop of ultrapure water then observed under light microscopy at ×100 and ×1,000 magnification. For epifluorescence microscopy, filaments were stained with SYBR Green I (ref. [30]) and observed with a Zeiss Axioskop 2 microscope. Micrographs were analysed with FIJI–ImageJ[31] to measure the sheath and trichome diameters.

CARD-FISH analysis. Domain-level taxonomic affiliation of prokaryotes associated with Venus's hair filaments was assessed by CARD-FISH analysis[32,33]. Briefly, Venus's hair filaments were hand-picked from basanite samples and suspended in PBS buffer, then centrifuged and further suspended in 1:1 solution of PBS buffer:96% ethanol. Samples were diluted, filtered onto 0.2 µm filters and dipped in low-gelling point agarose (0.1% (wt/vol) in Milli-Q water), then dried on Petri dishes at 37 °C and dehydrated in 95% ethanol. Cell wall permeabilization was optimized by incubation at 37 °C with lysozyme for Bacteria or proteinase K for Archaea[34]. After washing with Milli-Q and incubation in 10 mM HCl (room temperature, 20 min), the filters were washed again, dehydrated in 95% ethanol, dried and hybridized with Horseradish Peroxidase (HRP)-labelled oligonucleotide probes: either Eub-mix (Eub338, Eub338-II and Eub338-III) to target Bacteria or Arch915 to target Archaea. The absence of non-specific signals was checked through the use of the NON-338 probe. Hybridization (35 °C for Bacteria, 46 °C for Archaea) was performed for 2 h. The filters were then transferred into preheated washing buffer, placed in PBS buffer (pH 7.6, 0.05% Triton X-100) and incubated at room temperature for 15 min. After removal of the buffer, samples were incubated for 30 min in the dark at 37 °C for Cy3-tyramide signal amplification. Filters were observed under epifluorescence microscopy.

SEM–EDX spectroscopy. Lava rock fragments colonized by the Venus's hair were analysed using SEM–EDX. Each fragment was fixed with a 2.5% paraformaldehyde–4% glutaraldehyde mix, incubated for 20 min and then thoroughly washed twice with PBS buffer. Fragments were dehydrated in ethanol at increasing concentrations (50%, 75%, 90%, 95% and 100% twice, each step for 15 min) and placed in a Petri dish for further desiccation using hexamethyldisilazane (HMDS). Samples were then placed on an aluminium stub and sputter-coated in gold-palladium before the SEM visualization[35,36].

TXRF analysis. Venus's hair filaments were hand-picked with a sterile steel pick under a Zeiss stereomicroscope and placed on a support disc for the TXRF analysis. Before the analysis, cells within filaments were counted under light microscopy. Gallium standard solution (0.5 mg l^{-1}) was added to the filaments and slowly homogenized. The sample was air dried and subsequently analysed with an S2 PICOFOX analyser[37]. Results were normalized to the number of cells counted.

Extracellular enzymatic activities. The extracellular enzymatic activities were determined by analysis of the cleavage rates of the artificial fluorogenic substrates, L-leucine-4-methylcoumarinyl-7-amide (Leu-MCA), 4-methylumbelliferyl-β-D-glucopyranoside (Glu-MUF) and 4-MUF-P-phosphate (MUF-P), for aminopeptidase, β-glucosidase and alkaline phosphatase, respectively[38]. Filaments were diluted with 4 ml of 0.2 µm prefiltered seawater collected at the water–sediment interface and added to the different artificial fluorogenic substrates. Samples were then incubated in the dark at the *in situ* temperature for 1 to 3 h. Fluorescence of the samples was measured immediately after the addition of the substrate and after incubation; for this, the samples were centrifuged (×3,000 *g*, 10 min) and the supernatant was analysed fluorometrically, at 380 nm excitation and 440 nm emission wavelengths for Leu-MCA, and at 365 nm excitation and 455 nm emission for Glu-MUF and MUF-P. The fluorescence was converted into enzymatic activity using standard curves of 7-amino-4-methylcoumarin for Leu-MCA and 4-methylumbelliferone for both Glu-MUF and MUF-P[39].

Metazoan extraction and analysis. A portion of the solidified lava rock with the attached filaments was sampled using an ROV, placed in hermetically closed jars and transported to the laboratory. The samples were treated with ultrasound to detach associated organisms. Extracted organisms were fixed in formalin and stained with Rose Bengal for microscopy analyses[40].

DNA extraction and sequencing. DNA extracted from single filaments picked with a sterile stainless steel pick was used for metagenomic analysis. Filaments were placed in 1 ml of sterile Milli-Q water before the extraction and purification of DNA, which was carried out using the PowerSoil DNA Kit (MO BIO Laboratories), according to the manufacturer's instructions.

DNA extracted from the entire microbial mat attached to the rock substrate was used for amplicon sequencing of bacterial and archaeal 16S rRNA and eukaryotic 18S rRNA genes, obtained through polymerase chain reaction analyses using specific primer sets[40,41]. Rock fragments covered by the mat (a few cm^3 each) were used for DNA extraction by directly immersing them in the extraction buffer provided by the Mo Bio PowerSoil DNA extraction kit, according to the manufacturer's instructions.

The DNA extracted from both the single filaments and the amplicons was sequenced on an Illumina MiSeq platform using V3 technology, producing 300 bp long paired-end sequences. Sequencing was carried out by LGC Genomics. For metagenomic sequencing, a whole MiSeq run was used (yielding a total of 28,318,895 paired-end sequences). For amplicon sequencing, each amplification reaction was run separately and then pooled on a single run (yielding 473,488 paired-end sequences for the bacterial primer pair, 8,484 paired-end sequences for the archaeal primer pair and 318,048 paired-end sequences for the eukaryotic primer pair).

Bioinformatic analyses. Bacterial and archaeal 16S rDNA sequences were first pooled together and paired-end pairs merged with FLASH[42] using the default parameters before undergoing quality trimming with PRINSEQ (discarding sequences shorter than 200 bp and removing sequences with a mean quality

score of 20)[43]. High-quality sequences were compared with those belonging to amplicon sequencing investigations related to marine vent sites worldwide and available in the National Center for Biotechnology Information (NCBI) database (Supplementary Table 4) using the QIIME pipeline[44] to create an OTU table, with the open-reference OTU picking procedure and to align sequences along the SILVA dataset[45]. All the available datasets created using 454 Roche Life Sciences or Illumina sequencing platforms that spanned the V2–V4 16S rDNA region were included in the comparison. Samples whose sequences did not cluster into OTUs alongside the others or which contributed less than 1,000 sequences to the comparison were discarded. Among the samples considered, were those from the Mid-Atlantic Ridge, Juan de Fuca Ridge and Guaymas Basin vents, and seawater samples collected above and around the Tagoro's eruption area. The core microbiome and phylogenetic distance calculation were computed using the same pipeline. Results of the alignment were visualized with the R 'ggplot2' package.

Sequences from the shotgun metagenomic run of filament-associated prokaryotes were merged with FLASH[42] using the default parameters before undergoing quality trimming with USEARCH (using a maximum *E* error of 0.75 and discarding sequences shorter than 100 bp)[46]. Trimmed, high-quality sequences were assembled with Newbler 2.6 on the iPlant platform (with the '–large' flag). The resulting sequence and quality files were combined with PRINSEQ[43] and trimmed to remove contig portions with a mean quality below 20, yielding 216,479 contigs. Subsequently, initial paired-end reads were mapped to the final contigs with BBMap (http://sourceforge.net/projects/bbmap/). The resulting.bam file was used to create a depth profile for the MetaBAT automated binner[47,48], which was used to successfully bin the contigs with the '–very sensitive' flag. The content and putative phylogenomic assignment of each bin was assessed by the CheckM tool[49]. Bins with a completeness percentage in excess of 80% and contamination percentage less than 10% were kept for further analyses.

Outliers in guanine–cytosine content and tetranucleotide frequencies, as well as sequences carrying multiple-copy genes, were removed[49]. To further remove potential contamination, bins were manually examined by using the VizBin[50] tool, which allowed visualization of the distribution of contigs longer than 1,000 bp in each bin according to their pentanucleotide signatures[50]. Contigs not closely clustering with the main bins were removed. Unbinned contigs and incomplete or contaminated bins were pooled together before undergoing a second mapping, binning and finishing run. Lastly, contigs with strong (>500 bit score) hits to the nt database not related to the main phylogenetic assignment (carried out with Megablast)[51] were removed.

Phylogenomic comparison. To compare the partial genomes obtained from metagenomic analyses of single filaments with genomes or partial genomes available in databases, we carried out a phylogenomic analysis with the PhyloPhlAn tool[52]. Briefly, genomic sequences of bacteria belonging to the same lineages identified for our partial genomes by the CheckM tool (for example, filamentous Thiotrichales for the bin 11, Chromatiales for the bin 14, Campylobacterales for the bin 6) and others used as outgroups were downloaded from the NCBI repository. The genomic sequences used for comparison also included those of bacteria from marine vent ecosystems (for example, Candidatus *Ruthia magnifica* and Candidatus *Vesicomyosocius okutanii*). The draft genome of *Thioploca araucae* Tha-CCL was also reconstructed by downloading raw reads from the NCBI repository (accession number PRJNA19383), which were quality-trimmed using PRINSEQ[43] to remove low-quality sequences ($Q<20$), assembled using MEGAHIT[53] and cleaned with VizBin[50]. Proteins were predicted from all downloaded genomes and genomic bins with the 'prodigal' tool[54] and were used as an input for the final phylogenomic analysis.

Analysis of the functional potential of genomic bins. Assessment of the functional potential for each genomic bin was carried out by mapping predicted proteins to the KEGG database. Proteins detected by the 'prodigal' tool were pooled together and analysed with the GhostKOALA tool to investigate the central and energy metabolic pathways[55].

The proteome of bin 11 was predicted using the tool CheckM[49]. Predicted proteins were also re-analysed by both the BlastKOALA tool, to investigate the central and energy metabolic pathways[55], and single DIAMOND searches on the nr database[56], to refine the affiliations and functions of specific proteins belonging to sulfur and nitrogen metabolism. Analyses of average nucleotide identities and average amino acid identities were carried out using an online calculator provided by the Kostas Lab website[57]. Further confirmation of the phylogenetic assignment was carried out using the Kaiju webserver[58], to assess the taxonomic affiliation of the contigs within the genome bin 11 against the complete set of bacterial and archaeal genomes.

Protein prediction was carried out using the 'prodigal' tool on the filament-associated metagenome, as well as from other hydrothermal vent-related assembled metagenomes (Supplementary Table 3). The cross-proteome comparisons were carried out with the USEARCH tool[46] using a local search, a minimal identity percentage of 0.7 and a maximum *E*-value of 10^{-5} to identify a hit.

Comparison among metagenomes. The filament-associated metagenome was compared with metagenomes from different vent ecosystems worldwide. For the comparison, we also included metagenomes from deep-sea sediment samples (Marmara Sea) and surface seawater samples (Fernandina Island), which we used as outliers. Raw sequencing reads (Supplementary Table 3) were downloaded from the NCBI and MG-RAST databases, and compared using the simka pipeline[59]. The resulting distance matrix was used to construct a neighbour-joining tree with the 'ape' R package.

Data availability. All sequences are publicly available under the sequence read archive (SRA) project PRJNA381123.

Received 10 August 2016; accepted 20 March 2017; published 24 April 2017

References

1. Smith, D. K. & Cann, J. R. The role of seamount volcanism in crustal construction at the Mid-Atlantic Ridge (24°–30° N). *J. Geophys. Res.* **97,** 1645–1658 (1992).
2. Rubin, K. H. *et al.* Volcanic eruptions in the deep sea. *Oceanography* **25,** 142–157 (2012).
3. Rivera, J. *et al.* Construction of an oceanic island: insights from El Hierro 2011–12 submarine volcanic eruption. *Geology* **41,** 355–358 (2013).
4. Fraile-Nuez, E. *et al.* The submarine volcano eruption at the island of El Hierro: physical–chemical perturbation and biological response. *Sci. Rep.* **2,** 486 (2012).
5. Santana-Casiano, J. M. *et al.* The natural ocean acidification and fertilization event caused by the submarine eruption of El Hierro. *Sci. Rep.* **3,** 1140 (2013).
6. Ferrera, I. *et al.* Effects of the submarine volcanic eruption of El Hierro (Canary Islands) on the bacterioplankton communities of the surrounding. *PLoS ONE* **10,** e0118136 (2014).
7. Gulmann, L. K. *et al.* Bacterial diversity and successional patterns during biofilm formation on freshly exposed basalt surfaces at diffuse-flow deep-sea vents. *Front. Microbiol.* **6,** 901 (2015).
8. Meyer, J. L., Akerman, N. H., Proskurowski, G. & Huber, J. A. Microbiological characterization of post-eruption "snowblower" vents at Axial Seamount, Juan de Fuca Ridge. *Front. Microbiol.* **4,** 153 (2013).
9. Emerson, D. & Moyer, C. L. Neutrophilic Fe-oxidizing bacteria are abundant at the Loihi Seamount hydrothermal vents and play a major role in Fe oxide deposition. *Appl. Environ. Microbiol.* **68,** 3085–3093 (2002).
10. Garcia, M., Caplan-Auerbach, J., De Carlo, E., Kurz, M. D. & Becker, N. Geology, geochemistry and earthquake history of Lō`ihi seamount, Hawai`i's youngest volcano. *Chem. Erde Geochem.* **66,** 81–108 (2006).
11. de Ronde, C. E. *et al.* Evolution of a submarine magmatic-hydrothermal system: Brothers volcano, southern Kermadec arc, New Zealand. *Econ. Geol.* **100,** 1097–1133 (2005).
12. Baker, E. T. *et al.* Hydrothermal activity and volcano distribution along the Mariana arc. *J. Geophys. Res.* **113,** B8 (2008).
13. Kelley, D. S., Baross, J. A. & Delaney, J. R. Volcanoes, fluids, and life at mid-ocean ridge spreading centers. *Annu. Rev. Earth Planet. Sci.* **30,** 385–491(2002).
14. Rivera, J. *et al.* Morphometry of Concepcion Bank: evidence of geological and biological processes on a large volcanic seamount of the Canary Islands Seamount Province. *PLoS ONE* **11,** e0156337 (2016).
15. Pérez-Torrado, F. J. *et al.* La erupción submarina de La Restinga en la isla de El Hierro, Canarias: Octubre 2011–Marzo 2012. *Estud. Geol.* **68,** 5–27 (2012).
16. Santana-Casiano, J. M. *et al.* Significant discharge of CO_2 from hydrothermalism associated with the submarine volcano of El Hierro Island. *Sci. Rep.* **6,** 25686 (2016).
17. Jørgensen, B. B. & Gallardo, V. A. *Thioploca* spp.: filamentous sulfur bacteria with nitrate vacuoles. *FEMS Microbiol. Ecol.* **28,** 301–313 (1999).
18. Preisler, A. *et al.* Biological and chemical sulfide oxidation in a Beggiatoa inhabited marine sediment. *ISME J.* **1,** 341–353 (2007).
19. Kojima, H. *et al.* Ecophysiology of *Thioploca ingrica* as revealed by the complete genome sequence supplemented with proteomic evidence. *ISME J.* **9,** 1166–1176 (2015).
20. Klatt, J. M. & Polerecky, L. Assessment of the stoichiometry and efficiency of CO_2 fixation coupled to reduced sulfur oxidation. *Front. Microbiol.* **6,** 484 (2014).
21. Albareda, M. *et al.* Dual role of HupF in the biosynthesis of [NiFe] hydrogenase in *Rhizobium leguminosarum*. *BMC Microbiol.* **12,** 256 (2012).
22. Stewart, F., Dmytrenko, O., DeLong, E. & Cavanaugh, C. Metatranscriptomic analysis of sulfur oxidation genes in the endosymbiont of *Solemya velum*. *Front. Microbiol.* **2,** 134 (2011).
23. Sanders, J. G., Beinart, R. A., Stewart, F. J., Delong, E. F. & Girguis, P. R. Metatranscriptomics reveal differences in *in situ* energy and nitrogen metabolism among hydrothermal vent snail symbionts. *ISME J.* **7,** 1556–1567 (2013).
24. Hügler, M. & Sievert, S. M. Beyond the Calvin cycle: autotrophic carbon fixation in the ocean. *Ann. Rev. Mar. Sci.* **3,** 261–289 (2011).

25. Oulas, A. *et al.* Metagenomic investigation of the geologically unique Hellenic Volcanic Arc reveals a distinctive ecosystem with unexpected physiology. *Environ. Microbiol.* **18,** 1122–1136 (2016).
26. Kirchman, D. L. The ecology of Cytophaga–Flavobacteria in aquatic environments. *FEMS Microbiol. Ecol.* **39,** 91–100 (2002).
27. Klatt, J. M. *et al.* Structure and function of natural sulphide-oxidizing microbial mats under dynamic input of light and chemical energy. *ISME J.* **10,** 921–933 (2016).
28. Van Gaever, S. *et al.* Trophic specialisation of metazoan meiofauna at the Håkon Mosby mud volcano: fatty acid biomarker isotope evidence. *Mar. Biol.* **156,** 1289–1296 (2009).
29. Tchesunov, A. V. Free-living nematode species (Nematoda) dwelling in hydrothermal sites of the North Mid-Atlantic Ridge. *Helgoland Mar. Res.* **69,** 343 (2015).
30. Noble, R. T. & Fuhrman, J. A. Use of SYBR Green I for rapid epifluorescence counts of marine viruses and bacteria. *Aquat. Microb. Ecol.* **14,** 113–118 (1998).
31. Schindelin, J. *et al.* Fiji: an open-source platform for biological-image analysis. *Nat. Methods* **9,** 676–682 (2012).
32. Pernthaler, A., Pernthaler, J. & Amann, R. Fluorescence *in situ* hybridization and catalyzed reporter deposition for the identification of marine bacteria. *Appl. Environ. Microbiol.* **68,** 3094–3101 (2002).
33. Teira, E., Reinthaler, T., Pernthaler, A., Pernthaler, J. & Herndl, G. J. Combining catalyzed reporter deposition-fluorescence *in situ* hybridization and microautoradiography to detect substrate utilization by bacteria and archaea in the deep ocean. *Appl. Environ. Microbiol.* **70,** 4411–4414 (2004).
34. Molari, M. & Manini, E. Reliability of CARD-FISH procedure for enumeration of Archaea in deep-sea surficial sediments. *Curr. Microbiol.* **64,** 242–250 (2012).
35. Hazrin-Chong, N. H. & Manefield, M. An alternative SEM drying method using hexamethyldisilazane (HMDS) for microbial cell attachment studies on sub-bituminous coal. *J. Microbiol. Meth.* **90,** 96–99 (2012).
36. Fischer, C. B., Rohrbeck, M., Wehner, S., Richter, M. & Schmeißer, D. Interlayer formation of diamond-like carbon coatings on industrial polyethylene: thickness dependent surface characterization by SEM, AFM and NEXAFS. *Appl. Surf. Sci.* **271,** 381–389 (2013).
37. Ratti, S., Knoll, A. H. & Giordano, M. Grazers and phytoplankton growth in the oceans: an experimental and evolutionary perspective. *PLoS ONE* **8,** e77349 (2013).
38. Hoppe, H. G. in *Handbook of Methods in Aquatic Microbial Ecology* (eds Kemp, P. F. *et al.*) 423–431 (CRC, 1993).
39. Corinaldesi, C., Tangherlini, M., Luna, G. M. & Dell'Anno, A. Extracellular DNA can preserve the genetic signatures of present and past viral infection events in deep hypersaline anoxic basins. *Proc. R. Soc. B* **281,** 20133299 (2014).
40. Danovaro, R. *Methods for the Study of Deep-Sea Sediments, their Functioning and Biodiversity* (CRC, 2010).
41. Klindworth, A. *et al.* Evaluation of general 16S ribosomal RNA gene PCR primers for classical and next-generation sequencing-based diversity studies. *Nucleic Acids Res.* **41,** e1 (2012).
42. Magoč, T. & Salzberg, S. L. FLASH: fast length adjustment of short reads to improve genome assemblies. *Bioinformatics* **27,** 2957–2963 (2011).
43. Schmieder, R. & Edwards, R. Quality control and preprocessing of metagenomic datasets. *Bioinformatics* **27,** 863–864 (2011).
44. Caporaso, J. G. *et al.* QIIME allows analysis of high-throughput community sequencing data. *Nat. Methods* **7,** 335–336 (2010).
45. Pruesse, E., Peplies, J. & Glöckner, F. O. SINA: accurate high-throughput multiple sequence alignment of ribosomal RNA genes. *Bioinformatics* **28,** 1823–1829 (2012).
46. Edgar, R. C. Search and clustering orders of magnitude faster than BLAST. *Bioinformatics* **26,** 2460–2461 (2010).
47. Kang, D. D., Froula, J., Egan, R. & Wang, Z. MetaBAT, an efficient tool for accurately reconstructing single genomes from complex microbial communities. *PeerJ* **3,** e1165 (2015).
48. Evans, P. N. *et al.* Methane metabolism in the archaeal phylum Bathyarchaeota revealed by genome-centric metagenomics. *Science* **350,** 434–438 (2015).
49. Parks, D. H., Imelfort, M., Skennerton, C. T., Hugenholtz, P. & Tyson, G. W. CheckM: assessing the quality of microbial genomes recovered from isolates, single cells, and metagenomes. *Genome Res.* **25,** 1043–1055 (2015).
50. Laczny, C. C. *et al.* VizBin—an application for reference-independent visualization and human-augmented binning of metagenomic data. *Microbiome* **3,** 1 (2015).
51. Altschul, S. F., Gish, W., Miller, W., Myers, E. W. & Lipman, D. J. Basic local alignment search tool. *J. Mol. Biol.* **215,** 403–410 (1990).
52. Segata, N., Börnigen, D., Morgan, X. C. & Huttenhower, C. PhyloPhlAn is a new method for improved phylogenetic and taxonomic placement of microorganisms. *Nat. Commun.* **4,** 2304 (2013).
53. Li, D., Liu, C. M., Luo, R., Sadakane, K. & Lam, T. W. MEGAHIT: an ultra-fast single-node solution for large and complex metagenomics assembly via succinct de Bruijn graph. *Bioinformatics* **31,** 1674–1676 (2015).
54. Hyatt, D. *et al.* Prodigal: prokaryotic gene recognition and translation initiation site identification. *BMC Bioinformatics* **11,** 19 (2010).
55. Kanehisa, M., Sato, Y. & Morishima, K. BlastKOALA and GhostKOALA: KEGG tools for functional characterization of genome and metagenome sequences. *J. Mol. Biol.* **428,** 726–731 (2016).
56. Buchfink, B., Xie, C. & Huson, D. H. Fast and sensitive protein alignment using DIAMOND. *Nat. Methods* **12,** 59–60 (2015).
57. Rodriguez-R, L. M. & Konstantinidis, K. T. Bypassing cultivation to identify bacterial species. *Microbe* **9,** 111–118 (2014).
58. Menzel, P., Ng, K. L. & Krogh, A. Fast and sensitive taxonomic classification for metagenomics with Kaiju. *Nat. Commun.* **7,** 11257 (2016).
59. Benoit, G. *et al.* Multiple comparative metagenomics using multiset k-mer counting. Preprint at https://arxiv.org/abs/1604.02412 (2016).

Acknowledgements

This work was carried out within the frame of the project MIDAS (GA n. 603418, EU FPVII) for which the Ministerio de Economía y Competitividad (MINECO) and Instituto Español de Oceanografía (IEO) provided ship time and the ROV. Technical staff were provided by IEO and Consejo Superior de Investigaciones Científicas (CSIC) Unidad de Tecnología Marina. Generalitat de Catalunya supported Grup de Recerca Consolidat (GRC) en Geociències Marines through grant 2014 SGR 1068. We thank the crew and officers of the RV *Ángeles Alvariño* for their help during the cruise. A.S.-V. was supported by a Ramón y Cajal contract from MINECO. R.D. was supported by the project MERCES (Marine Ecosystem Restoration in Changing European Seas, EU2020, grant agreement no. 689518). D.A. was supported by the European Union's Horizon 2020 research and innovation programme under the Marie Skłodowska-Curie grant agreement no. 658358.

Author contributions

R.D. and M.C. conceived the study. M.C., G.L. and A.M.C. led the research cruise where the Venus's hair mats were found, and mapped and sampled them. J.R. played a pivotal role in the ROV operations. M.T., D.A., J.F., R.P. and X.R. performed the fieldwork. A.S.-V. performed the substrate rock analyses. M.T., A.D.A. and C.C. carried out the bioinformatic analyses. C.G. performed the extraction and classification of the meiofaunal organisms. C.C., A.D.A. and M.T. conducted the laboratory analyses. R.D., M.C., C.C., A.D.A., C.G. and M.T. wrote the manuscript. G.L., A.S.-V and A.M.C. critically read and contributed to the manuscript.

Additional information

Supplementary information is available for this paper.

Reprints and permissions information is available at www.nature.com/reprints.

Correspondence and requests for materials should be addressed to R.D.

How to cite this article: Danovaro, R. *et al.* A submarine volcanic eruption leads to a novel microbial habitat. *Nat. Ecol. Evol.* **1,** 0144 (2017).

Publisher's note: Springer Nature remains neutral with regard to jurisdictional claims in published maps and institutional affiliations.

Competing interests

The authors declare no competing financial interests.